Ratcheting of the substrate from the zymogen to proteinase conformations directs the sequential cleavage of prothrombin by prothrombinase

Elsa P. Bianchini*, Steven J. Orcutt*, Peter Panizzi†, Paul E. Bock†, and Sriram Krishnaswamy*‡§

*Joseph Stokes Research Institute, Children's Hospital of Philadelphia, Philadelphia, PA 19104; ‡Department of Pediatrics, University of Pennsylvania, Philadelphia, PA 19104; and †Department of Pathology, Vanderbilt University, Nashville, TN 37232

Prothrombinase catalyzes thrombin formation by the ordered cleavage of two peptide bonds in prothrombin. Although these bonds are likely ≈36 Å apart, sequential cleavage of prothrombin at Arg-320 to produce meizothrombin, followed by its cleavage at Arg-271, are both accomplished by equivalent exosite interactions that tether each substrate to the enzyme and facilitate presentation of the scissile bond to the active site of the catalyst. We show that impairing the conformational transition from zymogen to active proteinase that accompanies the formation of meizothrombin has no effect on initial cleavage at Arg-320 but inhibits subsequent cleavage at Arg-271. Full thermodynamic rescue of this defective mutant was achieved by stabilizing the proteinase-like conformation of the intermediate with a reversible, active site-specific inhibitor. Irreversible stabilization of intact prothrombin in a proteinase-like state, even without prior cleavage at Arg-320, also enhanced cleavage at Arg-271. Our results indicate that the sequential presentation and cleavage of the two scissile bonds in prothrombin activation is accomplished by substrate bound either in the zymogen or proteinase conformations. The ordered cleavage of prothrombin by prothrombinase is driven by ratcheting of the substrate from the zymogen to the proteinase-like states.

blood coagulation | enzymology | proteolytic cleavage | serine protease | zymogen activation

Thrombin (IIa) is produced in a pivotal reaction of the blood coagulation cascade by specific proteolysis of prothrombin at two sites (1). The membrane-assembled prothrombinase complex is considered the physiologically relevant catalyst for this reaction (1, 2). Prothrombinase acts on the two scissile bonds through sequential cleavage reactions in an apparently ordered fashion. Provided that membrane binding by prothrombin is not compromised, prothrombin is cleaved after Arg-320 to yield meizothrombin¶ (mIIa) as an intermediate, followed by subsequent cleavage at Arg-271 to produce IIa (3, 4). The molecular bases for these findings remain obscure.

Because both cleavage sites in the zymogen appear accessible to proteolysis, prothrombin can be converted to thrombin by two possible cleavage pathways (3–6). Substrates for each of the four possible half-reactions in prothrombin activation bind prothrombinase in a mutually exclusive fashion and with equivalent affinity (4, 7). Three of the four possible reactions exhibit identical catalytic efficiencies, whereas cleavage at Arg-271 in intact prothrombin proceeds with a V_{max} that is ≈30-fold lower (4). These findings establish the quantitative basis for preferential cleavage at Arg-320 over Arg-271 in intact prothrombin and the largely ordered cleavage pathway that ensues (4). They fail, however, to provide an explanation for why a difference in V_{max}, and not affinity, drives selective recognition of the Arg-320 bond in intact prothrombin or why initial cleavage at Arg-320 greatly enhances the V_{max} for subsequent cleavage at Arg-271 without also affecting substrate affinity.

Substrate recognition in each of the four possible half-reactions is accomplished by an initial, active site-independent interaction with an extended surface (exosite) on prothrombinase, followed by active site engagement by the substrate and cleavage (8). Exosite binding is the principal determinant of substrate affinity, whereas the subsequent active site docking step contributes to the V_{max} (8). Cleavage of two scissile bonds is likely accomplished by a single exosite interaction that tethers the substrate to prothrombinase and presents structures flanking each cleavage site to the catalyst for active site docking (9). Because the two scissile bonds are expected to be separated by ≈36 Å in intact prothrombin, geometric constraints arising from exosite tethering might be expected to both facilitate and restrict active site docking of elements flanking each scissile bond with the active site of prothrombinase (4). Ordered cleavage and bond selectivity associated with differences in V_{max} could result from presentation constraints associated with substrate bound in one of two configurations to prothrombinase (4, 8).

Initial cleavage at Arg-320 converts prothrombin, the zymogen, to the serine proteinase mIIa (10). Abundant x-ray crystallographic evidence developed with members of the S1 family of serine proteinases exhibiting a chymotrypsin fold has established the mechanism(s) by which cleavage at this site results in conformational transitions and the conversion of the zymogen to the proteinase (11–14). The zymogen and proteinase could represent two distinct substrate conformations that are relevant to the action of prothrombinase on prothrombin. We have investigated the role of the zymogen to proteinase transition in determining the ordered presentation and cleavage of the two scissile bonds required for the conversion of prothrombin to thrombin.

Experimental Procedures

Reagents. The inhibitors D-phenylalanyl-L-prolyl-L-arginine chloromethyl ketone (FPR-CH₂Cl, Calbiochem) and dansyl-L-arginine N-(3-ethyl-1,5-pentanediyl)amide (DAPA, Hematologic Technologies, Essex, VT) were obtained from the indicated sources. The peptidyl substrate, H-D-phenylalanyl-L-pipecolyl-L-arginine-P-nitroanilide (S2238), was from Chromogenix. Small unilamellar phospholipid vesicles (PCPS) composed of 75% (wt/wt) hen egg L-α-phosphatidylcholine and 25% (wt/wt) porcine brain L-α-phosphatidylserine (Avanti Polar Lipids) were

---

BIOCHEMISTRY

prepared and characterized as described in ref. 15. Factors Xa and Va were prepared from factors X and V purified from human plasma and quality controlled as described in refs. 3, 4, and 16. A fragment comprising residues 1–325 of staphylocoagulase containing an additional Met at the NH_2 terminus and a His tag at fused to the COOH terminus (Met-SC$_{1-325}$-His-6) was prepared by modification of an expression construct described in ref. 13. Deletion of a stop codon allowed translation of an additional Lys-Leu-Ala-Ala-Ala-Leu-Glu-His-6 sequence at the COOH terminus. Met-SC$_{1-325}$-His-6 was expressed as described in ref. 13 and purified by affinity chromatography by using Ni^{2+}-iminodiacetic acid Sepharose (Amersham Pharmacia). Unless otherwise stated, kinetic studies were performed in 20 mM Hepes/0.15 M NaCl/5 mM Ca^{2+}/0.1% (wt/vol) PEG 8000, pH 7.4 (assay buffer) at 25°C. Extinction coefficients (E_{280} mg^{-1}·cm^2) and molecular weights (M_r) used to determine protein concentrations were Xa: 1.16, 45,300 (17); Va: 1.78, 173,000 (18); Met-SC$_{1-325}$-His-6: 1.00, 38,000; and all recombinant prothrombin variants: 1.47, 72,000 (4).

Recombinant Prothrombin Variants. Procedures for the expression and characterization of recombinant wild-type human II (II$_{WT}$) and II containing Gln in place of Arg-320 (II$_{Q320}$), have been described in ref. 4. The cDNA encoding human II was used as a template for mutagenesis by using the QuikChange mutagenesis kit (Stratagene) to replace codons encoding Ile-321-Val-322-Glu-323 with codons for Thr-Ala-Thr (II$_{TAT}$, II containing Thr-Ala-Thr after Arg-320) and to replace codons for Arg-155 and Arg-284 with codons for Gln (II$_{Q155,Q284}$, thrombin-resistant variant of II containing Gln in place of Arg-155 and Arg-284). The Gateway system (Invitrogen) was used to transfer the cassette encoding the prothrombin variants to an adapted pCDNA 3.1 (+) vector as described in ref. 4, and the integrity of each cassette was established by DNA sequencing. Transfection of HEK293 cells, selection of stable cell lines, large-scale expression, and purification of II$_{TAT}$ and II$_{Q155,Q284}$ were performed as described in ref. 4. NH_2-terminal sequencing and quantitative determination of γ-carboxyglutamic acid content, as described in refs. 4 and 19, established a correctly processed NH_2-terminal sequence and a full complement of γ-carboxyglutamic acid residues for each prothrombin variant (data not shown).

Preparation of FPR-II$_{Q320}$. Conformational activation of II$_{Q320}$ and its covalent inactivation with FPR-CH$_2$Cl was accomplished by the addition of 43 μM Met-SC$_{1-325}$-His-6 to a reaction mixture equilibrated at 25°C containing 25 μM II$_{Q320}$ and 250 μM FPR-CH$_2$Cl in 140 mM Hepes/76 mM NaCl/11% (vol/vol) glycerol, pH 7.8. Conformationally activated II$_{Q320}$ was ≈99% inhibited after 10 min, as measured by initial rates of S2238 hydrolysis. The incubation was continued for an additional 75 min, and the Met-SC$_{1-325}$-His-6·FPR-II$_{Q320}$ complex was captured by application to a column of Ni^{2+}-iminodiacetic acid-Sepharose equilibrated in 50 mM Hepes/400 mM NaCl/50 mM imidazole/10 μM FPR-CH$_2$Cl, pH 7.4. II$_{Q320}$ covalently modified with FPR-CH$_2$Cl after conformational activation (FPR-II$_{Q320}$) was eluted with 50 mM Hepes/125 mM NaCl/3 M NaSCN, pH 7.4, dialyzed against 50 mM Hepes/125 mM NaCl, pH 7.4, and separated from trace amounts of Met-SC$_{1-325}$-His-6/FPR-II$_{Q320}$ complex by chromatography on tandem Superdex 200 HR 10/30 columns (Amersham Pharmacia) equilibrated in the same buffer. FPR-II$_{Q320}$ free of Met-SC$_{1-325}$-His-6, eluting in the second of two peaks, was pooled, snap-frozen, and stored at −70°C. Residual uninhibited II$_{Q320}$ was estimated at ≈0.5%, as determined from the rate of S2238 hydrolysis after incubation of 100 nM FPR-II$_{Q320}$ with a staphylocoagulase fragment comprising residues 1–325 (250 nM) for 20 min at 25°C. A control substrate was prepared by treating II$_{Q320}$ with 3 M NaSCN for

2 h at room temperature, followed by gel filtration into 50 mM Hepes/0.11 M NaCl/5 mM Ca^{2+}/0.1% (wt/vol) PEG 8000, pH 7.4 and dialysis into 50 mM Hepes/125 mM NaCl, pH 7.4 before freezing. Both II$_{Q320}$ and FPR-II$_{Q320}$ were thawed and diluted into 35 mM Hepes/0.15 M NaCl/2 mM Ca^{2+}/0.1% (wt/vol) PEG 8000, pH 7.4 before use.

Kinetics of Bond Cleavage in Prothrombin Variants. Reaction mixtures prepared in assay buffer and maintained at 25°C, contained 5.4 μM II$_{WT}$, II$_{TAT}$, or II$_{Q155,Q284}$, 20 μM PCPS, 28 nM Va, and indicated concentrations of DAPA. Cleavage was initiated by the addition of 0.8 nM Xa and samples (15 μl), withdrawn at the indicated times, were quenched by mixing with an equal volume of 2× NuPAGE LDS sample buffer (Invitrogen) containing 50 mM EDTA. Quenched samples were treated with 71 mM DTT, heated at 89°C for 5 min, and subjected to electrophoresis (4.2 μg protein per lane) by using NuPAGE 4–12% gels and Mes running buffer (Invitrogen). Protein bands visualized by staining with Coomassie brilliant blue R-250 were imaged and analyzed by quantitative densitometry by using procedures described in detail in refs. 4 and 15. Analysis of the cleavage of FPR-II$_{Q320}$ and NaSCN-treated II$_{Q320}$ was performed as described above except that reaction mixtures contained 5.8 μM prothrombin variant, 50 μM PCPS, 60 nM Va, 40 μM DAPA, and 1 nM Xa. In all cases, representative findings are presented from two or more experiments performed at a comparable level of detail.

Binding of DAPA to Thrombin Variants. Front face fluorescence measurements were performed in a plate reader (SpectraMax Gemini, Molecular Devices) by using black polystyrene plates (no. 3650, Corning). Reaction mixtures (100 μl) prepared in assay buffer contained increasing concentrations of DAPA (24 concentrations, 0–100 μM) with no addition, 0.5 μM IIa, or 0.5 μM IIa$_{TAT}$. Fluorescence intensity was determined by integrating emission spectra between 510 and 530 nm at 25°C by using $λ_{EX}$ = 280 nm with a 495-nm long-pass filter in the emission beam. Subtraction of the intensity measured with DAPA alone yielded the fluorescence change associated with the binding of DAPA to IIa or IIa$_{TAT}$. Fluorescence data were analyzed as described in ref. 7 to infer the equilibrium dissociation constant.

Results

Activation-Defective Variant of Prothrombin. Initial cleavage of prothrombin at Arg-320 reveals a new NH_2-terminal sequence (Ile-Val-Glu) that is essential for the formation of an internal salt bridge. Salt bridge formation induces conformational changes in the proteinase domain and maturation of the active serine proteinase (11, 13, 20). We prepared a recombinant prothrombin derivative (II$_{TAT}$) in which the Ile-Val-Glu sequence was replaced with Thr-Ala-Thr, normally found after the Arg-271 cleavage site. The intent was to produce a prothrombin variant that could be cleaved normally but with impaired ability to undergo the conformational transition to active proteinase after cleavage at Arg-320. Accordingly, II$_{TAT}$ could be fully converted to IIa$_{TAT}$[∥] after prolonged digestion with prothrombinase (see below). Although correct cleavage at Arg-320 was verified by NH_2-terminal sequencing, purified IIa$_{TAT}$ exhibited only ≈0.2% of the specific activity of wild-type IIa as determined by initial velocity measurements with 100 μM S2238 (data not shown).

Kinetics of Prothrombin Cleavage. Cleavage of II$_{WT}$ by prothrombinase yielded bands established to arise from the sequential cleavage at Arg-320, yielding mIIa as the sole intermediate, followed by cleavage at Arg-271 to produce IIa (4). Prothrombin disappearance was accompanied by the transient appearance of

---

[∥]mIIa$_{TAT}$ and IIa$_{TAT}$ refer to mIIa and IIa produced from II$_{TAT}$.
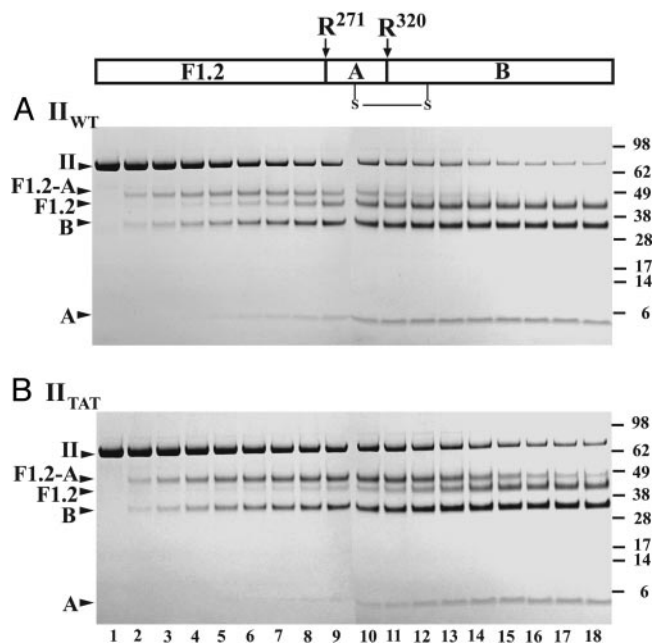
Fig. 1. Cleavage of prothrombin variants by prothrombinase. The indicated prothrombin derivatives (5.4 μM) were digested by 0.8 nM prothrombinase (0.8 nM Xa/28 nM Va/20 μM PCPS). II$_{WT}$ (*A*) was activated in the presence of 60 μM DAPA, and II$_{TAT}$ (*B*) was activated in the absence of DAPA. Serially quenched samples were analyzed by SDS/PAGE (4.2 μg per lane) after disulfide bond reduction. Lanes 1–18 correspond to reaction times of 0, 0.33, 0.67, 1, 1.33, 1.67, 2, 2.5, 3, 3.5, 4, 6, 8, 12, 16, 20, 26, and 32 min. The margins indicate molecular weights (×10³) of the markers and the migration positions of relevant prothrombin fragments. The relationship between the two cleavage sites and the relevant prothrombin fragments is schematically illustrated at the top of the figure.

F1.2-A, uniquely associated with mIIa formation, followed by the delayed appearance of F1.2 and A chain of IIa, denoting IIa production (Fig. 1*A*). Cleavage of II$_{WT}$ has been established to be qualitatively and quantitatively indistinguishable from the cleavage of prothrombin isolated from plasma (4). An equivalent banding pattern and key diagnostic features of the reaction profile observed with II$_{TAT}$ (Fig. 1*B*) implicated the same order of bond cleavage in this variant. However, although II$_{TAT}$ disappeared in a way that was comparable with II$_{WT}$, the band

arising from mIIa$_{TAT}$ produced after initial cleavage at Arg-320 was more intense and persisted throughout the time course. Bands arising from IIa$_{TAT}$ produced by the second cleavage reaction at Arg-271 appeared more slowly (Fig. 1*B*).

Quantitative densitometry yielded a reaction profile for II$_{WT}$ cleavage that was consistent with the sequential conversion of II$_{WT}$ to mIIa, followed by its cleavage at Arg-271, to produce IIa (Fig. 2*A*). Initial rates of consumption of II$_{WT}$ and II$_{TAT}$, resulting from cleavage at Arg-320, were comparable and differed only by ≈15% (Fig. 2). The lower extent of II$_{TAT}$ consumption most likely reflects the results of product inhibition by the accumulating intermediate. For either substrate, mIIa was produced at the same initial rate. However, mIIa$_{TAT}$ accumulated to a greater extent and decayed slowly, with significant amounts evident even after 30 min, whereas IIa$_{TAT}$ was produced at a slower rate (Fig. 2*B*). Additional data points extending to 120 min established quantitative conversion of II$_{TAT}$ to IIa$_{TAT}$ (data not shown).

Studies of II$_{WT}$ cleavage require the use of DAPA, a tight-binding inhibitor of IIa and mIIa, to prevent feedback cleavages in the substrate and intermediate (Figs. 1*A* and 2*A*). DAPA was not present in studies with II$_{TAT}$ (Figs. 1*B* and 2*B*). Differences in the cleavage of II$_{WT}$ and II$_{TAT}$ could reflect an unexpected effect of DAPA unrelated to the sequence after the Arg-320 cleavage site. This possibility was eliminated by the results of studies with and without DAPA by using II$_{Q155,Q284}$, a thrombin-resistant variant (Fig. 3). The reaction profile for II$_{Q155,Q284}$ cleavage by prothrombinase was comparable with that observed for the cleavage of II$_{WT}$ both in the presence and absence of 60 μM DAPA (Fig. 3).

The data indicate that mutation of the residues after the Arg-320 cleavage site and the associated impairment in proteinase formation has minimal impact on the first cleavage reaction at Arg-320 but produces a distant effect on subsequent cleavage at Arg-271. Integration of the area under the progress curve for mIIa formation (extending to 120 min) suggests that the second cleavage reaction is ≈20-fold slower in II$_{TAT}$ than in II$_{WT}$ or in II$_{Q155,Q284}$.

Rescue of II$_{TAT}$ Cleavage by DAPA. In contrast to the findings with II$_{Q155,Q284}$, DAPA significantly altered product profiles of II$_{TAT}$ cleavage without detectably influencing bond cleavage order. DAPA had a minor effect on II$_{TAT}$ consumption (Fig. 4). Increasing concentrations of DAPA, as high as 300 μM, did not significantly affect the initial rate of mIIa$_{TAT}$ formation but
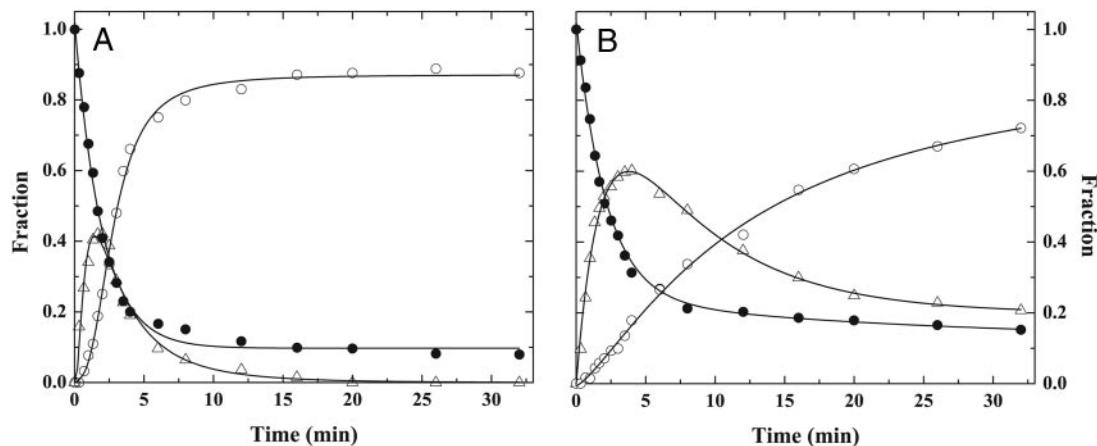

Fig. 2. Reaction profiles for the action of prothrombinase on II$_{WT}$ and II$_{TAT}$. Progress curves for reactants and products in the activation of II$_{WT}$ with 60 μM DAPA (*A*) or II$_{TAT}$ in the absence of DAPA (*B*) were obtained by quantitative densitometry. Curves illustrate the disappearance of II (●), the transient formation of mIIa (△), and the accumulation of IIa (○). The lines were arbitrarily drawn.
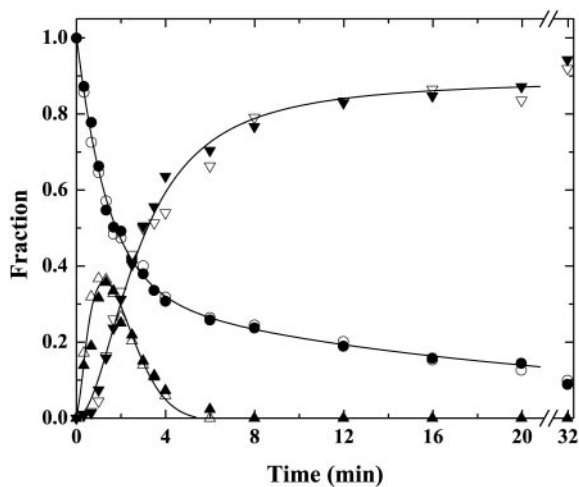
Fig. 3. Effect of DAPA on the cleavage of $II_{Q155,Q284}$. SDS/PAGE and quantitative densitometry for the activation of $II_{Q155,Q284}$ (5.4 μM) with 0.8 nM prothrombinase (0.8 nM Xa/31 nM Va/20 μM PCPS) in the absence of DAPA (open symbols) or in the presence of 60 μM DAPA (filled symbols). The disappearance of II ($\bigcirc$ and $\bullet$), the transient formation of mIIa ($\triangle$ and $\blacktriangle$) and the accumulation of IIa ($\triangledown$ and $\blacktriangledown$) are illustrated. The lines were arbitrarily drawn.

decreased the amplitude of $mIIa_{TAT}$ production and increased the rate of IIa_{TAT} formation (Fig. 4). At saturating concentrations of DAPA, progress curves for $mIIa_{TAT}$ and IIa_{TAT} resembled those obtained in the activation of II_{WT}. The observations indicate that DAPA has a minimal effect on the initial cleavage of II_{TAT} at Arg-320 but can rescue defective cleavage at Arg-271. This rate-enhancing effect of DAPA on Arg-271 cleavage is specific to the action of prothrombinase on II_{TAT}.

Effects of DAPA were assessed by integrating areas under the progress curves for mIIa formation and its disappearance for the different prothrombin variants (Fig. 5). Normalized areas obtained in the activation of II_{WT} or $II_{Q155,Q284}$ were identical and were independent of DAPA varied between 0 and 300 μM for $II_{Q155,Q284}$ or 20 and 300 μM for II_{WT}. In the case of II_{TAT}, the integrated area (obtained by integration to 120 min) was $\approx$20-fold higher in the absence of DAPA and decreased saturably to values observed with II_{WT} (Fig. 5). Thus, a defective second half-reaction in II_{TAT} cleavage is fully rectified by high concentrations of DAPA with a half-maximal effect at $\approx$20 μM.

Although DAPA is established to act as a tight-binding, active site-directed inhibitor of IIa and mIIa ($K_d \approx 1$ nM) (21), the data imply a far weaker interaction between DAPA and $mIIa_{TAT}$ or IIa_{TAT}. Fluorescence studies assessing the binding of DAPA to IIa_{WT} were consistent with a nanomolar equilibrium dissociation constant (data not shown). Although the amplitude of the fluorescence change observed with IIa_{TAT} and saturating concentrations of DAPA was comparable with that observed with IIa_{WT}, DAPA bound weakly to purified IIa_{TAT} with $K_d = 31.7 \pm 2.3$ μM (data not shown). This dissociation constant is in agreement with the concentration of DAPA required to observe 50% rescue of II_{TAT} cleavage (Fig. 5).

One interpretation of the results is that the full rescue of Arg-271 cleavage in II_{TAT} by high concentrations of DAPA arises from its weak interaction with $mIIa_{TAT}$ and the thermodynamic stabilization of a proteinase-like state in an otherwise zymogen-like $mIIa_{TAT}$ species produced after the initial cleavage at Arg-320. This interpretation implies that effective presentation of structures flanking the Arg-271 site to the active site of prothrombinase requires a substrate in a proteinase-like configuration.
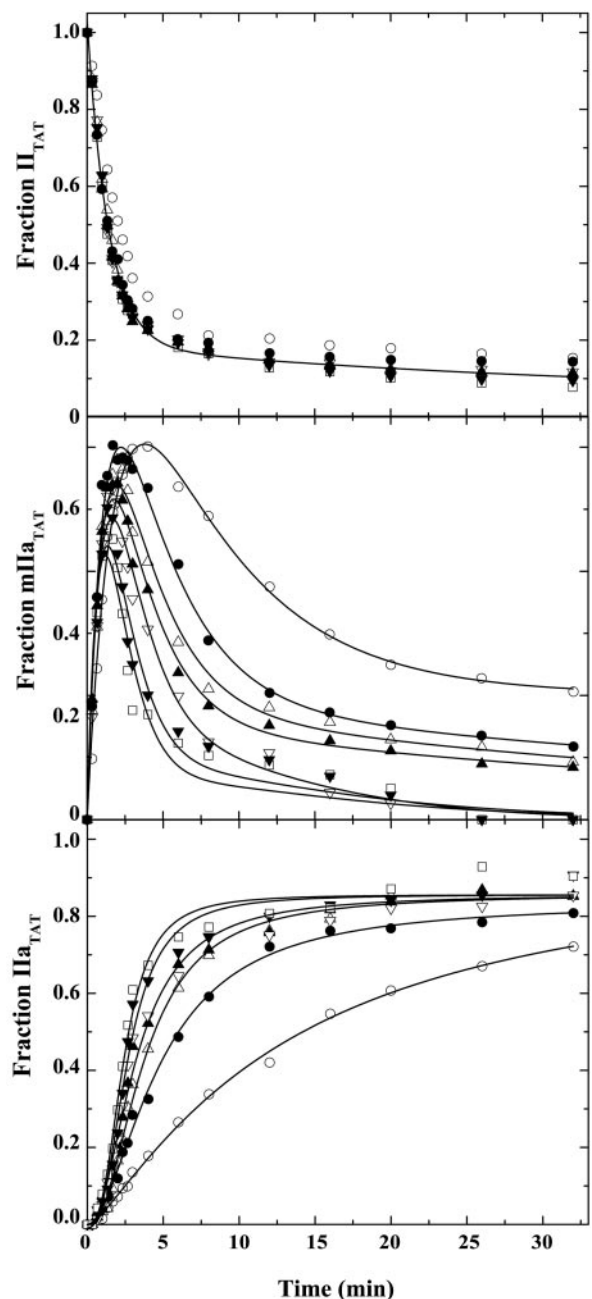

Fig. 4. Modulation of II_{TAT} cleavage by DAPA. II_{TAT} (5.4 μM) was activated by 0.8 nM prothrombinase (0.8 nM Xa/28 nM Va/20 μM PCPS) in the presence of 0 ($\bigcirc$), 20 μM ($\bullet$), 40 μM ($\triangle$), 60 μM ($\blacktriangle$), 100 μM ($\triangledown$), 200 μM ($\blacktriangledown$), and 300 μM ($\square$) DAPA. Progress curves, obtained by SDS/PAGE and quantitative densitometry, illustrate the fates of II_{TAT} (*Top*), $mIIa_{TAT}$ (*Middle*), and IIa_{TAT} (*Bottom*). Additional data points extending to 120 min have been omitted for clarity. All lines were arbitrarily drawn.

Stabilization of the Uncleaved Zymogen in a Proteinase-Like State. Prior work with a prothrombin variant (II_{Q320}) containing a single cleavable site at Arg-271 has established that the Arg-271 site in the intact zymogen is cleaved slowly by prothrombinase (4). In agreement, analysis by SDS/PAGE and quantitative densitometry showed slow cleavage at Arg-271 in II_{Q320} (Fig. 6). FPR-II_{Q320} was produced by conformational activation of II_{Q320} with Met-SC$_{1-325}$-His-6, covalent inactivation of the complex with FPR-CH$_2$Cl, followed by dissociation and separation from Met-SC$_{1-325}$-His-6. FPR-II_{Q320} is an uncleaved prothrombin an-
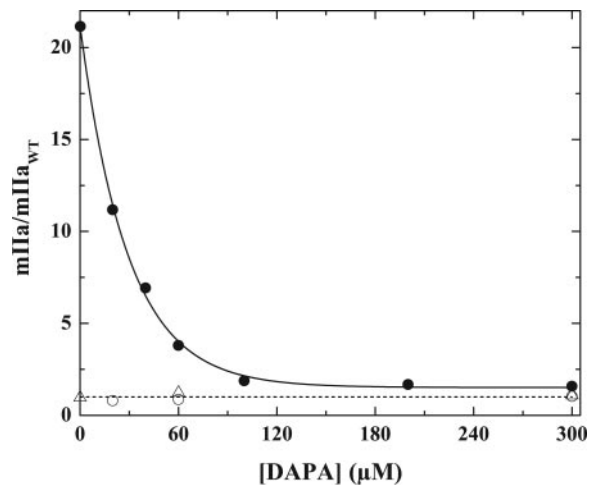
Fig. 5. Effect of DAPA on meizothrombin accumulation. Total meizothrombin accumulation in the cleavage of II_{WT} (○), II_{TAT} (●), and $II_{Q155,Q284}$ (△) as a function of increasing concentrations of DAPA was estimated by integrating areas under progress curves and normalizing the value to the area under the mIIa progress curve with II_{WT} measured at 60 μM DAPA. The dashed line denotes a value of 1. The solid line was arbitrarily drawn.

alog that is expected to be stabilized in a more proteinase-like state by the inhibitor covalently bound to the active site. Cleavage at Arg-271 in FPR-II_{Q320} by prothrombinase was enhanced ≈12-fold in comparison with cleavage at the same site in II_{Q320} (Fig. 6). Thus, stabilization of the substrate in a proteinase-like state, even without cleavage at Arg-320, enhances presentation and cleavage at Arg-271.

Discussion

Our observations, along with the mechanisms established for substrate recognition by prothrombinase (8), are consistent with the interpretations outlined in Scheme 1. Exosite-dependent tethering of the substrate to prothrombinase in either the zymogen or the proteinase configurations is proposed to govern presentation of the individual cleavage sites for docking to the active site of the catalyst and cleavage (Scheme 1). Active site docking of the Arg-320 site is facilitated when the substrate is
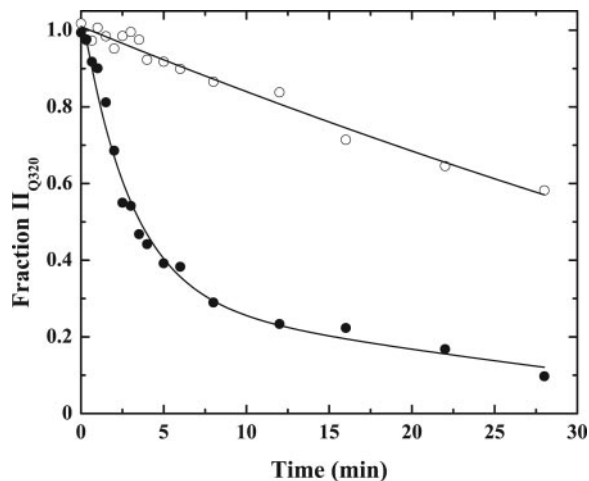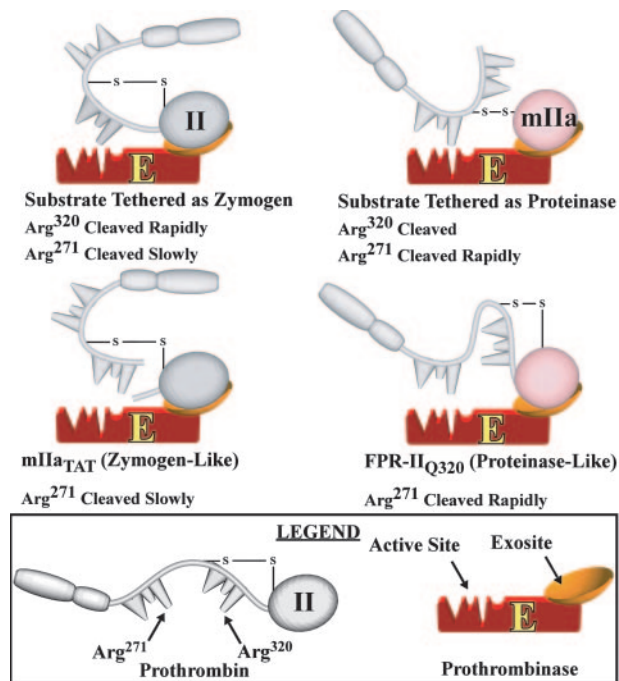

Fig. 6. Cleavage at Arg-271 in the uncleaved zymogen. Prothrombin derivatives (5.8 μM) were digested with 1 nM prothrombinase (1 nM Xa/60 nM Va/50 μM PCPS) in the presence of 40 μM DAPA. The fraction of II_{Q320} (○) and FPR-II_{Q320} (●) remaining as a function of time was determined by SDS/PAGE and quantitative densitometry. The lines were arbitrarily drawn.

Scheme 1. Substrate bound to prothrombinase in either the zymogen or proteinase configurations. Substrate species in either the zymogen or proteinase states are illustrated to be bound to prothrombinase through exosite interactions. For clarity, only the different forms of such possible enzyme–substrate complexes are illustrated without additional steps reflecting substrate binding or intermediate dissociation.

bound in the zymogen configuration, whereas effective presentation of the Arg-271 site requires that the substrate is bound in the proteinase configuration after initial cleavage at Arg-320. These ideas provide an explanation, at the molecular level, for bond selectivity and the largely ordered action of prothrombinase on the two spatially distinct cleavage sites in prothrombin.

Selective impairment of the second cleavage reaction in the activation of II_{TAT} is proposed to reflect the suboptimal presentation of the Arg-271 site because of the zymogen-like configuration of mIIa$_{TAT}$ despite its prior cleavage at Arg-320 (Scheme 1). Conversely, forcing the zymogen to adopt a proteinase-like configuration yields enhanced presentation and cleavage at Arg-271 even without prior cleavage at Arg-320 (Scheme 1). Thus, the conformational transition of the substrate between zymogen and proteinase states plays a role in regulating the action of prothrombinase on the two cleavage sites in the protein substrate.

The structural basis for the conversion of zymogen to proteinase in the chymotrypsin-like serine proteinases fold has been established with numerous x-ray structures, including those for derivatives of II, mIIa, and IIa (10–14, 22). The Ile-Val-Glu NH_2 terminus generated after cleavage at Arg-320 inserts into the NH_2-terminal binding cleft in the catalytic domain and yields a salt bridge between Ile-321 (Ile^{C16})** and Asp^{C194}. Salt bridge formation triggers conformational changes in the so-called activation domains (11–14, 23, 24). These changes are associated with the formation of the substrate binding pocket and the oxyanion hole required for catalysis (11–14, 22). In the case of mIIa, these conformational changes could also be transmitted to the other domains that remain covalently attached (25). Because

---

**Residues in the proteinase domain, numbered according to the homologous residues in chymotrypsinogen (22), are denoted by a C preceding the residue number.

formation of the internal salt bridge depends on the NH_2-terminal sequence produced after cleavage at Arg-320, some or all of these linked changes are likely disrupted in mIIa$_{TAT}$ (11, 24). It is not possible to discern whether impaired cleavage at Arg-271 in mIIa$_{TAT}$, which we have ascribed to its zymogen-like nature, arises from all or a subset of the linked conformational changes associated with the zymogen to proteinase transition.

Full and specific rescue of the defect in II$_{TAT}$ cleavage by high concentrations of DAPA indicates that this active site-directed ligand somehow rectifies impaired docking of the Arg-271 cleavage site with the active site of prothrombinase in the otherwise zymogen-like mIIa$_{TAT}$ (Scheme 1). Ligands that bind with high affinity to the proteinase are established to enhance the ability of the zymogen to adopt a proteinase-like configuration (13, 20, 23). Our findings are consistent with two possible interpretations. DAPA could bind weakly ($K_d \approx 30$ μM) to the zymogen-like mIIa$_{TAT}$ and overcome a kinetic and/or thermodynamic barrier in its conversion to the proteinase-like state. Alternatively, DAPA could act by selectively binding and favoring the proteinase in an equilibrium between zymogen-like and proteinase-like forms of mIIa$_{TAT}$ in which the zymogen-like state is highly favored.

Effectively ordered cleavage of prothrombin by prothrombinase arises because Arg-271 in intact prothrombin is cleaved with a V_{max} that is $\approx$30-fold lower than for cleavage at Arg-320, and prior cleavage at Arg-320 increases the V_{max} for cleavage at Arg-271 by a factor of $\approx$30 (4). Provided the ideas outlined in Scheme 1 can fully explain the differential recognition of the two sites in prothrombin, blocking the conformational transition to proteinase is expected to maximally yield a $\approx$30-fold slower rate of cleavage at Arg-271, even after cleavage at Arg-320. Complete

stabilization of the zymogen in the proteinase state is expected to maximally yield a $\approx$30-fold enhancement in cleavage at Arg-271, even without prior cleavage at Arg-320. These boundary conditions, established by the kinetic constants measured for the individual cleavage reactions, are generally consistent with the magnitude of effects we have observed. The somewhat smaller enhancement ($\approx$12-fold) observed in Arg-271 cleavage in FPR-II$_{Q320}$ could reflect the possibility that this derivative has not been completely driven to a proteinase-like state. Nevertheless, taken together, the results illustrate that it is not cleavage at Arg-320 *per se* but the ensuing conformational change that facilitates subsequent cleavage at Arg-271.

Our findings now provide a comprehensive explanation for a range of kinetic findings and an explanation for how ordered cleavage of prothrombin is achieved. Ratcheting of the substrate from the zymogen to proteinase conformations drives the sequential presentation of the two cleavage sites to the active site of the catalyst leading to the ordered action of prothrombinase on prothrombin. These concepts may also have bearing on the mechanisms underlying the ordered action of proteinases at multiple sites in their protein substrates in coagulation and in other areas of biology.

1. Mann, K. G., Jenny, R. J. & Krishnaswamy, S. (1988) *Annu. Rev. Biochem.* **57,** 915–956.
2. Mann, K. G., Nesheim, M. E., Church, W. R., Haley, P. & Krishnaswamy, S. (1990) *Blood* **76,** 1–16.
3. Krishnaswamy, S., Church, W. R., Nesheim, M. E. & Mann, K. G. (1987) *J. Biol. Chem.* **262,** 3291–3299.
4. Orcutt, S. J. & Krishnaswamy, S. (2004) *J. Biol. Chem.* **279,** 54927–54936.
5. Esmon, C. T., Owen, W. G. & Jackson, C. M. (1974) *J. Biol. Chem.* **249,** 606–611.
6. Carlisle, T. L., Bock, P. E. & Jackson, C. M. (1990) *J. Biol. Chem.* **265,** 22044–22055.
7. Boskovic, D. S., Troxler, T. & Krishnaswamy, S. (2004) *J. Biol. Chem.* **279,** 20786–20793.
8. Krishnaswamy, S. (2005) *J. Thromb. Haemost.* **3,** 54–67.
9. Boskovic, D. S. & Krishnaswamy, S. (2000) *J. Biol. Chem.* **275,** 38561–38570.
10. Martin, P. D., Malkowski, M. G., Box, J., Esmon, C. T. & Edwards, B. F. (1997) *Structure (London)* **5,** 1681–1693.
11. Huber, R. & Bode, W. (1978) *Acc. Chem. Res.* **11,** 114–122.
12. Khan, A. R. & James, M. N. G. (1998) *Protein Sci.* **7,** 815–836.
13. Friedrich, R., Panizzi, P., Fuentes-Prior, P., Richter, K., Verhamme, I., Anderson, P. J., Kawabata, S., Huber, R., Bode, W. & Bock, P. E. (2003) *Nature* **425,** 535–539.
14. Vijayalakshmi, J., Padmanabhan, K. P., Mann, K. G. & Tulinsky, A. (1994) *Protein Sci.* **3,** 2254–2271.
15. Walker, R. K. & Krishnaswamy, S. (1994) *J. Biol. Chem.* **269,** 27441–27450.
16. Buddai, S. K., Toulokhonova, L., Bergum, P. W., Vlasuk, G. P. & Krishnaswamy, S. (2002) *J. Biol. Chem.* **277,** 26689–26698.
17. Di Scipio, R. G., Hermodson, M. A. & Davie, E. W. (1977) *Biochemistry* **16,** 5253–5260.
18. Toso, R. & Camire, R. M. (2004) *J. Biol. Chem.* **279,** 21643–21650.
19. Camire, R. M., Larson, P. J., Stafford, D. W. & High, K. A. (2000) *Biochemistry* **39,** 14322–14329.
20. Bode, W. (1979) *J. Mol. Biol.* **127,** 357–374.
21. Hibbard, L. S., Nesheim, M. E. & Mann, K. G. (1982) *Biochemistry* **21,** 2285–2292.
22. Bode, W., Mayr, I., Baumann, U., Huber, R., Stone, S. R. & Hofsteenge, J. (1989) *EMBO J.* **8,** 3467–3475.
23. Bode, W., Schwager, P. & Huber, R. (1978) *J. Mol. Biol.* **118,** 99–112.
24. Bode, W. & Huber, R. (1976) *FEBS Lett.* **68,** 231–236.
25. Chen, Q. & Lentz, B. R. (1997) *Biochemistry* **36,** 4701–4711.